JOURNAL OF THERMOPHYSICS AND HEAT TRANSFER
Vol. 10, No. 2, April–June 1996

Assessment of Schemes for Coupling Monte Carlo and Navier–Stokes Solution Methods

D. B. Hash* and H. A. Hassan†
North Carolina State University, Raleigh, North Carolina 27695-7910

A planar Couette flow is simulated using several different interface conditions in a hybrid technique in which the direct simulation Monte Carlo (DSMC) method and the Navier–Stokes equations are coupled. Comparison of computational times and accuracy of the different methods are made to determine the best approach for further study. It is concluded that the Marshak condition, in which the properties at the interfaces between the continuum and rarefied regions are determined from flux conservation equations, is the best technique in terms of accuracy and run-time performance. When coupling Navier–Stokes and DSMC solvers, the use of a Maxwellian distribution to represent the particle velocity distribution in the Navier–Stokes region yields unacceptable errors.

Nomenclature

A = interface cross-sectional area
c' = thermal speed, $c'^2 = u'^2 + v'^2 + w'^2$
F = half-flux
F_{num} = ratio of real-to-simulated particles
f = velocity distribution function
f_0 = Maxwellian distribution
h = plate separation
K = coefficient of thermal conductivity
Kn = Knudsen number, λ/h
Kn_l = local Knudsen number
k = Boltzmann constant
n = number density
P = pressure
q = heat flux
R = gas constant
T = temperature
U = mean velocity in x direction
u, v, w = particle velocities
v = particle velocity vector
β = reciprocal of the most probable thermal speed at equilibrium
ΔT = sampling time
λ = mean free path
μ = viscosity
ρ = density
τ = shear stress
ω = viscosity-temperature exponent
$\nabla\rho$ = gradient of density

Subscripts
ref = reference value
w = wall value

Superscripts
$'$ = thermal component
$-$ = average value

Presented as Paper 95-0410 at the AIAA 33rd Aerospace Sciences Meeting and Exhibit, Reno, NV, Jan. 9–12, 1995; received Jan. 30, 1995; revision received Sept. 5, 1995; accepted for publication Nov. 6, 1995.

*Graduate Research Assistant, Mars Mission Research Assistant. Member AIAA.

†Professor, Mars Mission Research Assistant. Associate Fellow AIAA.

Introduction

WHEN it comes to computing, faster is better as long as the accuracy of physical models is maintained. Efforts are underway to develop new methodologies and computer architectures to reduce computational times. Such attempts are especially important for simulations of rarefied gas flows. The most common tool used in this field is the direct simulation Monte Carlo (DSMC) method of Bird.[1] The method simulates the actual movement and collisions of the microscopic particles that compose a gas. The DSMC method is a very powerful tool that provides much more detailed information than any conventional continuum-type approach, e.g., the solution of the Navier–Stokes equations. Its main theoretical restriction is the assumption of binary collisions so that only dilute gases can be simulated. This is not an important restriction since most gases of interest for aerospace applications are dilute. Unfortunately, the method is comparatively more computationally intensive than continuum-type approaches.

For this reason, efforts are being made to combine the advantageously faster solutions of continuum approaches with the DSMC method in a hybrid format. In many applications involving rarefaction, the flowfields of interest are comprised of regions of both continuum and rarefaction. A perfect example of this is the flowfield surrounding a blunt body entering the upper atmosphere. For certain altitudes, the majority of the forebody flowfield can be represented by a continuum, while the wake exhibits a high degree of rarefaction. Other examples can be found in a variety of applications such as plume impingement studies, plasma processing, and microelectromechanical systems.

The premise of the hybrid approach is as follows. In the regions where the continuum assumption is valid, a Euler or Navier–Stokes solver is used. In the remaining portion, the DSMC technique is employed. Immediately, two important questions must be resolved: 1) how does one define the demarcator between continuum and noncontinuum, and 2) how are the solutions coupled?

Question of Demarcation

To answer the question of demarcation, one must determine a measure of the breakdown of the continuum assumption. This is typically associated with the presence of strong translational nonequilibrium as defined by Vincenti and Kruger.[2] Here, translational nonequilibrium refers simply to the departure from the equilibrium velocity distribution, the Maxwellian distribution. By this definition, any flow exhibiting viscous or heat transfer effects experiences a degree of translational non-

equilibrium. The breakdown of the continuum assumption usually coincides with a degree of translational nonequilibrium for which anisotropic pressure effects arise. Along these lines, Bird advocates a continuum breakdown parameter defined as $(U/\bar{c})(\lambda/\rho)|\nabla\rho|$, with a limit value between 0.01–0.02, or a limit of 0.1 based on a local Knudsen number defined by

$$Kn_l = (\lambda/\rho)|\nabla\rho| \tag{1}$$

For a hybrid approach, we have to be even more specific about the criterion for breakdown. We are interested in a definitive metric for when the Navier–Stokes equations are no longer accurate. With this in mind, Boyd et al.[3] carried out an extensive numerical investigation of one-dimensional normal shock waves and two-dimensional bow shocks comparing DSMC and Navier–Stokes results, to determine an appropriate breakdown criterion. They considered both the local Knudsen number approach and Bird's breakdown parameter. They concluded that the local Knudsen number provides a better indication of breakdown and that a value of 0.05 guarantees a discrepancy between the solutions of less than 5%. Another criterion has been espoused by Eggers and Beylich,[4] in which a combination of local Knudsen number and a measure of the perturbation of the velocity distribution from Maxwellian is used. The perturbation criterion is an approximation to the first two terms in the Chapman–Enskog expansion,[5] which include the effects of both temperature and velocity gradients. For the present research, the local Knudsen number approach is deemed sufficient, and its implementation will be detailed later in the discussion.

Hybrid Coupling

The second question, concerning the coupling of the solutions, is the crux of the hybrid problem. Coupling basically involves the determination of the properties at the interface between the DSMC and Navier–Stokes regions. The macroscopic properties are required by the Navier–Stokes equations for the evaluation of the net fluxes and are necessary for the DSMC method for the specification of the distribution functions used to initialize particles entering from the Navier–Stokes side into the DSMC region. Figure 1 illustrates a typical interface. The procedure takes the following form. First, the particles in the DSMC region are allowed to move and collide. If they cross the interface, they are removed. At the end of each hybrid time step, particles enter from the Navier–Stokes side, such that mass, momentum, and energy fluxes are conserved across the interface. This is accomplished through the coupling procedure in which the macroscopic interface properties, used to specify these particles, are determined. The coupling occurs at specified time increments, and the process is repeated until a steady state is reached and is continued while samples are accumulated for the DSMC region.

Just as there are many ways for answering the demarcation question, there are many methods for solving the coupling question. Four prevalent methods are 1) the Marshak condition, 2) the extrapolation of flow properties, 3) the extrapolation of net fluxes, and 4) the use of the asymptotic values of the solution of the linear kinetic half-space problem. The Marshak condition is the first documentable hybrid-coupling mechanism, suggested by Golse.[6] The condition is borrowed from the field of radiative heat transfer and involves the equating of the half-fluxes at the interface. By half-flux, we mean the flux of particles with velocities comprising only half of the normal velocity component range. The net flux is the sum of the incoming and outgoing half-fluxes. For the Marshak condition, the half-fluxes of mass, momentum, and energy of the particles crossing the interface during the DSMC step are measured. These half-fluxes are then added to the incoming half-fluxes from the Navier–Stokes side and equated with the net flux. When assuming a Maxwellian distribution for the Navier–Stokes emission, this gives five equations and five unknowns providing the macroscopic properties of density, velocity, and temperature at the interface. More detailed information concerning this research can be found in the work of Bourgat et al.[7–9] The second method of extrapolating flow properties was proposed by Wadsworth and Erwin[10,11] and involves extrapolation of the macroscopic properties of density, velocity, and temperature to the interface. The accuracy to which conservation is attained is dependent on the order of the extrapolation. Further work with this approach was carried out by Eggers and Beylich.[4,12] The third method is similar to the second. Finally, the fourth method involving a linear kinetic half-space problem was developed for the situation in which the Marshak condition is not valid and where severe translational nonequilibrium exists. Since the interfaces in the current investigation are defined in regions of slight translational nonequilibrium, i.e., small local Knudsen number, the final method is not necessary and is not investigated here. However, excellent descriptions of this method are given by Golse,[6] Illner and Neunzert,[13] and Klar.[14]

The purpose of the present investigation is to determine the physical and numerical advantages and disadvantages of the previously mentioned coupling conditions and to select one for further investigation. Studies are made to determine the effect of the number of simulated particles and the frequency of coupling on the computational times and physical accuracy. Because emphasis is placed on these issues, adaptive location of the interfaces is not examined in this work. Once determined, the interfaces remained fixed. All investigations are carried out for a planar Couette flow for a simple monatomic gas to make an efficient parametric study.

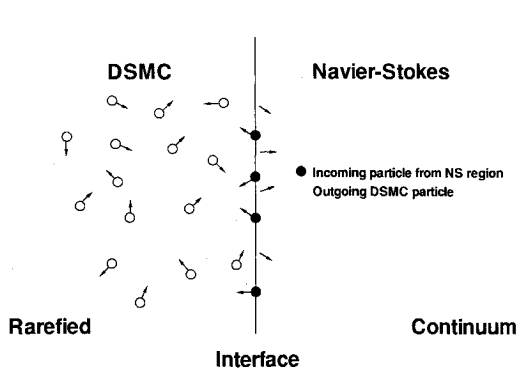

Fig. 1 Interface illustration.

Problem Definition

A planar Couette flow of argon gas is computed using the hybrid method. Both the DSMC and Navier–Stokes solvers use exactly the same gas models. A variable hard-sphere (VHS) model[1] is used, where the viscosity is given by

$$\mu/\mu_{\text{ref}} = (T/T_{\text{ref}})^{\omega} \tag{2}$$

and the thermal conductivity is written as $K = 15/4R\mu$ with μ_{ref}, T_{ref}, ω, and R equal to 2.117×10^{-5} kg/m·s, 273 K, 0.811, and 207.85 J/kg·K, respectively. The upper and lower plates of the Couette flow are maintained at a temperature of 273 K and are treated as fully diffuse. The lower plate is at rest while the upper plate moves with a velocity of 1000 m/s. The plate separation is 1 m.

The DSMC technique has been described previously and a general one-dimensional code published by Bird[1] was used in this work. The Navier–Stokes equations reduce to the following simple relations for the planar Couette flow:

$$P = \text{const}, \qquad \tau = \mu \frac{dU}{dy} = \text{const}$$
$$q + \tau U = K \frac{dT}{dy} + \mu U \frac{dU}{dy} = \text{const} \tag{3}$$

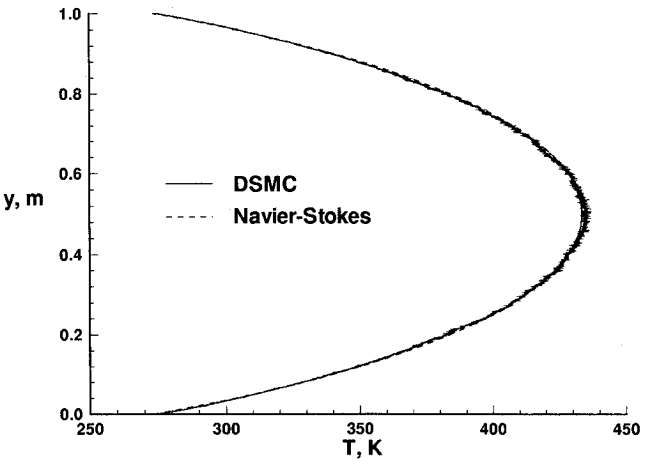

Fig. 2 Temperature profiles for $Kn = 0.0012$.

This is a system of two first-order ordinary differential equations (ODEs) and can be solved with a simple shooting method. The integration for the shooting method used a fourth-order Runge–Kutta scheme. Interestingly, the velocity and temperature profiles for the continuum planar Couette flow problem are not a function of pressure. In the presence of rarefaction, this will not be the case.

The consistency of the DSMC and Navier–Stokes methods is validated by simulating a continuum flowfield where the solutions should agree. For this case, a pressure of 7.53 N/m^2 and a nominal Knudsen number λ/h at the midsection of 0.0012 are employed. Any pressure large enough to provide a continuum flowfield could have been used since the velocity and temperature continuum profiles are not a function of pressure. The smallest pressure accomplishing this is desired for the DSMC method since the computational time is proportional to the number of particles simulated. A higher pressure means more simulated particles, which in turn, means longer computational times. The previously specified pressure produces a continuum flowfield with reasonable DSMC computational times. The resulting temperature profiles are depicted in Fig. 2. The profiles coincide, thereby substantiating the consistency of the two methods.

Hybrid Details for the Couette Flow

The simulation of a Couette flow greatly simplifies the hybrid problem. Only two interfaces will be required as depicted in Fig. 3. The core of the flow will be solved with the continuum approach, and the rarefied layers at each wall will be computed using the DSMC method. First, the entire flowfield is initialized by the full Navier–Stokes solution. The solution is used to determine the location of the interfaces and to initialize the particles in the newly defined DSMC regions. Once determined, the interface locations remained fixed. The continuum demarcator is chosen conservatively, i.e., a small value for the local Knudsen number criterion, 0.005, is used. In this way, if there are differences between the continuum and hybrid values for the interface local Knudsen number, the interfaces will still be located appropriately in regions of slight rarefaction.

This research concentrates on comparative analysis of different hybrid methods to determine the best for further study. This analysis is made without having adaptive interfaces to keep it simple and instructive.

As the solution evolves, the properties at the interface will be constantly updated. The Navier–Stokes region only requires values of velocity and temperature at each interface for the shooting method. The DSMC region requires more macroscopic properties to specify the distribution of particles entering from the Navier–Stokes side. In this investigation, a Chapman–Enskog procedure is used to specify this distribution. However, the effects of using a Maxwellian distribution will be examined. The Chapman–Enskog distribution function can be written as

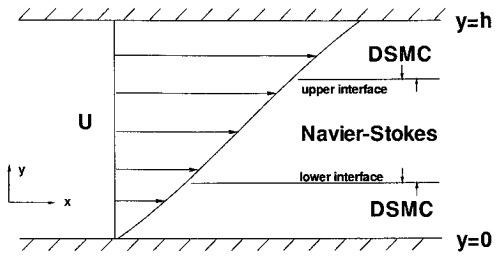

Fig. 3 Couette flow diagram.

$$f = f_0\left[1 - \frac{4K\beta^2}{5nk}(\beta^2 c'^2 - 5/2)c_i'\frac{\partial\, \ell n\, T}{\partial x_i} - \frac{4\mu\beta^4}{\rho}\left(c_i'c_j' - \frac{c'^2}{3}\delta_{ij}\right)\frac{\partial u_i}{\partial x_j}\right] \tag{4}$$

where

$$f_0 = (\beta^2/\pi)^{3/2}\exp(-\beta^2 c'^2) \qquad \beta^2 = 1/2RT \tag{5}$$

For a Couette flow with the velocity in the x direction, this simplifies to

$$f = f_0\left[1 - \alpha\left(\beta^2 c'^2 - \frac{5}{2}\right)v' - \gamma u'v'\right]$$
$$\alpha = \frac{6}{5}\frac{\mu R\beta^4}{\rho}\frac{\partial T}{\partial y}, \quad \gamma = \frac{4\mu\beta^4}{\rho}\frac{\partial U}{\partial y} \tag{6}$$

The parameters α and γ can be written in terms of a type of local Knudsen number, where

$$\frac{\alpha}{\beta} = \frac{45}{2\bar{\omega}}\frac{\lambda}{T}\nabla T, \qquad \frac{\gamma}{\beta^2} = \frac{60}{\bar{\omega}}\frac{\lambda}{\bar{c}'}\nabla U \tag{7}$$

with $\bar{\omega} = (5 - 2\omega)(7 - 2\omega)$. These parameters give a measure of how far the distribution is perturbed from Maxwellian and illustrate why the local Knudsen number criterion is useful for determining the interface locations. The second parameter λ/β^2 can be shown to equal $-2\pi/P$, which is a constant throughout the Couette flow and is not a useful interface criterion for the present investigation. Since the pressure is constant for the Couette flow, the first parameter α/β is proportional to the local Knudsen number defined in Eq. (1), which is used in this work as the continuum demarcator.

From the distribution in Eq. (6), we can derive the required distributions to specify the individual velocity components at each of the interfaces. The normal component distribution function, where the plane of interest is normal to the y axis, is given as

$$f_{v'} \propto \int_{-\infty}^{\infty}\int_{-\infty}^{\infty} v' f\, du'\, dw' \tag{8}$$

However, the other components must be integrated over the half-range. For example,

$$f_{u'} \propto \int_{-\infty}^{\infty}\int_{0}^{\infty} v' f\, dv'\, dw' \tag{9}$$

at the upper interface and

$$f_{u'} \propto \int_{-\infty}^{\infty}\int_{-\infty}^{0} v' f\, dv'\, dw' \tag{10}$$

at the lower interface, since we are only interested in particles crossing the interface. To prescribe the previous distributions, they must be normalized. The nonnormal components are normalized over the full velocity range, whereas the normal component is normalized over the half-range. Given this, the following results follow for the forward and backward distributions, respectively:

$$f_{\beta u'} = \left(\frac{1}{\sqrt{\pi}} \pm \frac{\alpha}{4\beta} \mp \frac{\alpha}{2\beta} x^2 \mp \frac{\gamma}{2\beta^2} x\right) \exp(-x^2), \quad x = \beta u'$$

$$f_{\beta v'} = \left(\pm 2x \pm 3\frac{\alpha}{\beta} x^2 \mp 2\frac{\alpha}{\beta} x^4\right) \exp(-x^2), \quad x = \beta v' \tag{11}$$

$$f_{\beta w'} = \left(\frac{1}{\sqrt{\pi}} \pm \frac{\alpha}{4\beta} \mp \frac{\alpha}{2\beta} x^2\right) \exp(-x^2), \quad x = \beta w'$$

The previous distribution functions are not necessarily nonnegative. This can easily be observed by considering the zeroes of the previous functions. Each function will cross the axis and become negative at some point. This is nonphysical and is a result of the approximate nature of the Chapman–Enskog expansion. It is not a concern as long as the zeroes occur close to infinity. Numerically, the particle thermal velocities must be specified with a finite range. Typically, this range is from $-3/\beta$ to $3/\beta$. Thermal velocities outside this range are highly unlikely and are neglected. For small gradients, α and γ, the distributions remain positive in the range of interest. Since the interfaces are defined such that the local Knudsen number is small, the interface gradients will be small, and concerns about negative values for the distributions are not warranted.

The previous distribution functions are used to determine the velocities of particles crossing an interface. Note that most of the previous implementations used Maxwellian distributions instead. To employ the distributions in Eq. (11), an acceptance–rejection method[15] is required, which involves the determination of the distribution maxima. Analytical expressions for these maximums can be attained for the nontangential components; the tangential component u' requires the solution of a cubic equation.

The following sections discuss in detail the specifics of each of the different hybrid techniques mentioned previously. All derivations and discussions relate specifically to the Couette flow under investigation.

Marshak Condition

The Marshak condition employs a conservation of fluxes at the interface. Here, the net flux is set to the half-flux crossing from the DSMC side plus the half-flux crossing from the Navier–Stokes side. The DSMC half fluxes are written as a summation over the simulated particles crossing the interface:

$$F_{\text{DSMC}} = \pm\frac{F_{\text{num}}}{A\Delta T}\sum_i \begin{bmatrix} 1 \\ m_i v_i \\ (m_i/2)(\mathbf{v}_i \cdot \mathbf{v}_i) \end{bmatrix} \tag{12}$$

where + is for the positive range half-flux, − is for the negative range half-flux, and i represents particles crossing the interface. For the Navier–Stokes side, the half-flux equations are as follows for the upper interface:

$$F_{\text{NS}} = n\int_{-\infty}^{\infty}\int_{0}^{\infty}\int_{-\infty}^{\infty} vQf\,du\,dv\,dw, \qquad Q = \begin{bmatrix} 1 \\ mv \\ (m/2)(\mathbf{v}\cdot\mathbf{v}) \end{bmatrix} \tag{13}$$

These equations reduce to the following for the Couette flow:

$$F_{\text{NS}} = \begin{bmatrix} \dfrac{n\bar{c}'}{4} \\ mNU + \dfrac{\tau}{2} \\ \dfrac{P}{2} + \dfrac{4}{5\pi}\dfrac{q}{\bar{c}'} \\ 0 \\ \dfrac{P\bar{c}'}{2} + \dfrac{\rho\bar{c}'U^2}{8} + \dfrac{q}{2} + \dfrac{\tau U}{2} \end{bmatrix} \tag{14}$$

Similar equations can be derived for the lower interface. Since the y and z mean velocities are zero, the previous equation, when added to Eq. (12) and equated to the net flux along with the equation of state, give us only five useful equations with six unknowns: P, T, ρ, U, τ, and q. This problem is not the typical Marshak problem as described earlier, because of the assumption of a Chapman–Enskog distribution for the Navier–Stokes emission. The system is underdetermined, and additional information is obtained from the solution of the Navier–Stokes equations in the form of the derivatives of U and T used to define two of the unknowns in the Marshak problem, q and τ. Moreover, the procedure for determining the properties at the interface will have to be an iterative one. Different methods for this iteration will be addressed in the Results section.

Extrapolation of Flow Properties

In this simple procedure, the DSMC solution is allowed to evolve while accumulating samples for the determination of macroscopic properties. After a specified number of time steps, the solution is stopped, and the velocity and temperature are evaluated. At the first coupling, initial guesses for the interface velocity and temperature are taken from the full Navier–Stokes solution. Subsequent initial guesses for the interface values are made using the values from the last coupling. The solution is obtained for the Navier–Stokes core. Then, the two solutions are smoothed around the interface region, and new values for the interface are obtained. The solution for the Navier–Stokes region is repeated, and this process iterated upon until the interface values converge. A good smoothing routine is required, and for this investigation a quadratic least-squares-fit of the profiles around the interfaces is employed. The smoothing region involved eight cells encompassing the interface. Higher-order fits were avoided because of the oscillations they can introduce. The derivatives necessary for the specification of the distribution functions are taken from the solution of the Navier–Stokes region at the interfaces.

Extrapolation of Net Fluxes

At first glance, this method may seem synonymous with the Marshak condition. However, the methods are quite different. The extrapolation of net fluxes in no way involves the measurement of half-fluxes at the interfaces. Instead, this method attempts to equate the net fluxes. The extrapolation of the net fluxes to the interface requires the evaluation of the shear stress and heat flux in each region. This is a simple task in the Navier–Stokes region involving the evaluation of numerical derivatives. These quantities in the DSMC region are evaluated from the thermal velocities as

$$\tau = \rho\overline{u'v'} \tag{15}$$

$$q = \tfrac{1}{2}\rho\overline{c'^2 v'} \tag{16}$$

Once these are determined, the net fluxes can be computed, and an average value can be obtained for the DSMC cells.

These net flux constants [see Eq. (3)] can then be used in the solution of the first-order ODEs for the Navier–Stokes region. The initial values are taken as the extrapolated velocity and temperature at the lower interface. Equation (3) can then be treated as an initial value problem. The main difficulty with the method is that the evaluation of the net flux constants must be very accurate to ensure that the calculated values at the upper interface conform with the profile predicted by the DSMC method in the upper region. In practice, the scatter in the higher moments indicated in Eqs. (15) and (16) is so great that the method is essentially useless.

Results

Kn = 0.003 Simulations

The first calculations were made for a slightly rarefied condition with a pressure of 2.95 N/m^2 and a midsection Knudsen number Kn of 0.003. The time step was 2.5×10^{-6} s, which was less than one-half of the mean collision time to ensure that the decoupling of the movement and collision is valid in the DSMC regions. The DSMC cells were less than one-quarter of the mean free path to adequately capture the flow gradients. The Navier–Stokes cells were 2.5 times larger than the DSMC cells that produced cell Reynolds numbers $\rho U \Delta y/\mu$ less than 2. Furthermore, the DSMC and Navier–Stokes solutions were coupled every 100 time steps.

The choice of the continuum demarcator is arbitrary and can only be determined by defining the tolerable discrepancy between the hybrid solution and the full DSMC solution. For this work, the demarcator was chosen as Kn_l = 0.005. This is a much stronger condition than suggested by Bird[1] or Boyd et al.[3] Here, the intent is to determine the numerical requirements of the hybrid code in terms of number of particles, frequency of coupling, etc. Thus, we want whatever discrepancy occurs to be because of these parameters and not because of an improper placement of the interfaces. Once the parameters required for the hybrid methods are found, other less stringent demarcators can be used. The conservative value of the local Knudsen number criterion placed the interfaces such that only 1% of the flow was simulated using the DSMC method. This simple case allowed very fast examination of the different methods and the parameters that affect them.

As stated previously, the Marshak condition as implemented in this work involved half-flux equations with six unknowns and five useful equations. Different approaches for closing this set of equations were tried. First, a derivative in the form of either the heat flux or the shear stress was taken from the Navier–Stokes solution at the interface. This involved making an initial guess for this gradient and then using it to determine the properties at the interface. Once the new properties were determined, the Navier–Stokes region was integrated, and a new gradient was determined. The new gradient was again used in the half-flux equations to determine new properties at the interface. This process was repeated until convergence was obtained. It was found that using only one of the gradients from the Navier–Stokes solution provided very poor results and introduced an unacceptable level of scatter. In the ensuing investigations, it was discovered that using both gradients and neglecting one of the half-flux equations provided very good results. In separate trials, either the number or the energy half-flux equation was neglected; both produced similar results. In retrospect, use of a conservative demarcator is somewhat necessary so as not to compromise heat flux and skin friction calculations.

Similar difficulties were observed with the method of extrapolating the net fluxes. This method was not feasible because of the level of scatter in the net fluxes, which for this problem are the shear stress and the heat flux plus viscous dissipation. The shear stress and heat flux are higher moments of the distribution function. A larger amount of scatter is associated with the higher moments than the first moments of

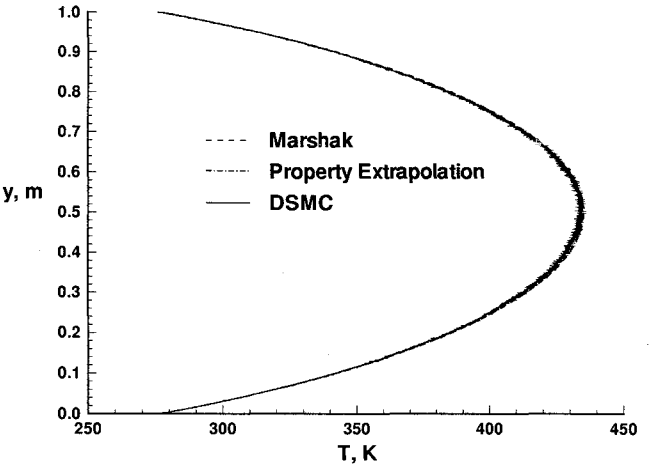

Fig. 4 Temperature profiles for Kn = 0.003.

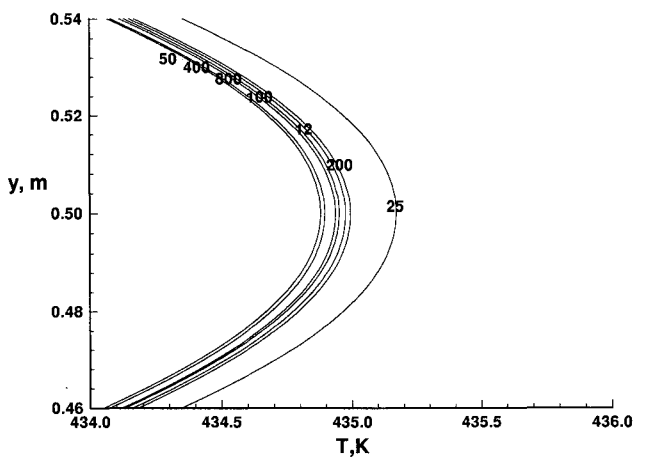

Fig. 5 Marshak solution variation with number of particles per cell.

velocity and temperature. The important conclusion from these investigations is that information concerning higher moments should not be obtained from the DSMC method in hybrid work. It is possible to determine them, but not without a large number of samples. Thus, the following research concentrates only on the Marshak condition using Navier–Stokes information for the shear stress and heat flux and the extrapolation of flow properties.

Figure 4 shows the results for the Marshak condition and the property extrapolation technique compared with the full DSMC results. Both methods compare well. Further work was undertaken to investigate the effect of the number of simulated particles used. Figures 5 and 6 depict the results for the Marshak condition and the property extrapolation methods, respectively. In each of these figures, the midsection region is focused on improving the clarity and better illustrating the variation with the number of particles. It appears from the figures that the property extrapolation technique is more sensitive to the number of particles simulated.

Comparative measurements of run times were made for this Knudsen number. All of the calculations were carried out on one 50-Mflop processor of a Silicon Graphics Challenge. Table 1 depicts the times required for 1000 time steps and 10 couplings for the different methods. These cases used an average of 100 particles per cell. As seen from the table, the Marshak condition represents a speed up of 43 as compared to the full DSMC solution. Such a dramatic result is to be expected, since only 1% of the flow is simulated with the DSMC method for the hybrid cases. Furthermore, the Marshak condition is 20% faster than the extrapolation technique. Extra work is required

Table 1 CPU for various methods, $Kn = 0.003$

Method	CPU, s	Total no. of simulated particles
Marshak	47.7	2,500
Property extrapolation	60.0	2,500
DSMC	2046.9	216,000

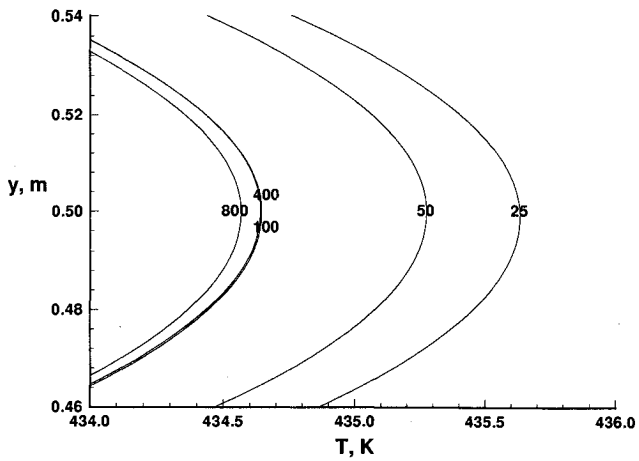

Fig. 6 Property extrapolation solution variation with number of particles per cell.

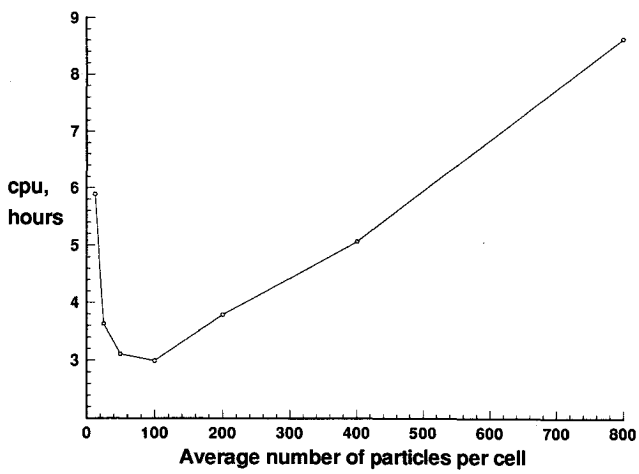

Fig. 7 Variation of Marshak CPU times with number of particles per cell.

by the extrapolation method because of the smoothing routine employed.

Figure 7 depicts the variation of run times with the average number of particles per cell for the Marshak cases. The same trend was seen for the extrapolation technique. The amount of time steps calculated after steady state was determined such that each case had eight million samples per cell. As seen from the figure, the quickest run times were acquired when using 100 particles per DSMC cell. Of course, the computational time spent for the transient decreases with the number of particles simulated. However, this has to be balanced with the time spent to calculate the steady state. With less particles, more time steps are required for the steady state to acquire the same accuracy. The use of 100 particles per cell represents the best balance between transient and steady-state computational times for this condition. This is not to say that this is the best choice for the number of simulated particles per cell for all situations, since this is most definitely a function of the flow conditions and the total number of particles simulated. However, for this case it is an advantageous result, providing increased accuracy with reduced computational time, as compared to using fewer particles.

Finally, the $Kn = 0.003$ case was used to determine the effect of specifying a Maxwellian distribution for the particles emitted from the Navier–Stokes region. Figure 8 displays the results of the simulation using the Marshak condition with a Chapman–Enskog and a Maxwellian distribution compared to the full DSMC simulation. The region near the wall around the interface is enlarged to best illustrate the results. As can be seen in the figure, the Maxwellian assumption does a poor job. This should not be surprising for the Couette flow, since it is driven purely by gradient effects. Omission of these effects in the distributions used for specifying the Navier–Stokes emission seriously degrades the performance of the hybrid code. Consequently, a Maxwellian distribution should not be used in the presence of translational nonequilibrium, i.e., viscous effects.

$Kn = 0.009$ Simulations

For further investigation, a pressure of 1.0 N/m^2 was chosen with a nominal Knudsen number of 0.009. Figure 9 shows the temperature profiles for the full Navier–Stokes and DSMC solutions for this Knudsen number. For the Navier–Stokes solution, 500 cells were used. This specification produced cell Reynold's numbers, $\rho U \Delta y/\mu$, less than 2, and provided 5-digit accuracy in the shear stress. The shear-stress accuracy was determined by investigating variations in the flowfield shear stress with the number of cells used. For the DSMC simulation, a time step of 4×10^{-6} s was used, guaranteeing that the time step was less than one-third of the mean collision time. Eight-hundred cells were used such that the cell sizes were less than one-quarter of the mean free path. The DSMC

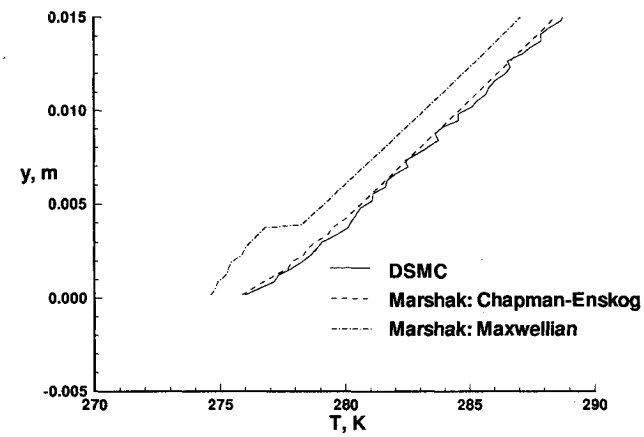

Fig. 8 Effect of Maxwellian for $Kn = 0.003$.

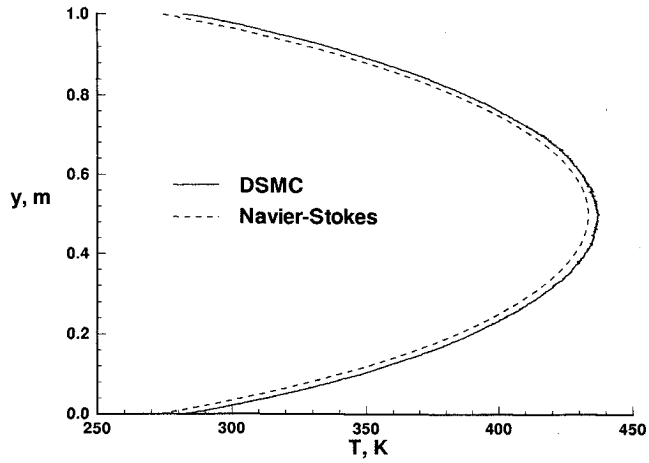

Fig. 9 Temperature profiles for $Kn = 0.009$.

solution was initialized with the Navier–Stokes solution and reached steady state after 0.4 s. To determine the steady state, solutions were obtained by starting the sampling of macroscopic properties in the DSMC method at different times. Once the solutions obtained from these investigations ceased to change, steady state was obtained. One-hundred-thousand samples were acquired to resolve the macroscopic properties. As seen in the figure, the profiles do not coincide. It is most likely that slip conditions would be an effective remedy for the discrepancy. However, the point of the present work is not to investigate the merits of slip conditions. Here, we are interested in the effectiveness of a hybrid code. More rarefied conditions could easily be employed for which slip conditions would be useless.

The hybrid cases used the same time step and cell spacings as the full DSMC and Navier–Stokes solutions in their respective regions. Once again, the conservative criterion of 0.005 for the local Knudsen number is used to determine the interface locations. For this case, they were located at approximately one- and three-quarters of the plate separation, such that 55% of the gap was simulated by the DSMC method. Initial calculations were conducted with the same frequency of couplings as the previous case. The results for both the Marshak and property methods are presented in Fig. 10, using 25 and 100 simulated particles per cell. The results are not convincing for either method and for either number of simulated particles. However, the Marshak results offer a more accurate solution. To improve the simulations, the frequency of coupling was increased from every 100 time steps to every 50.

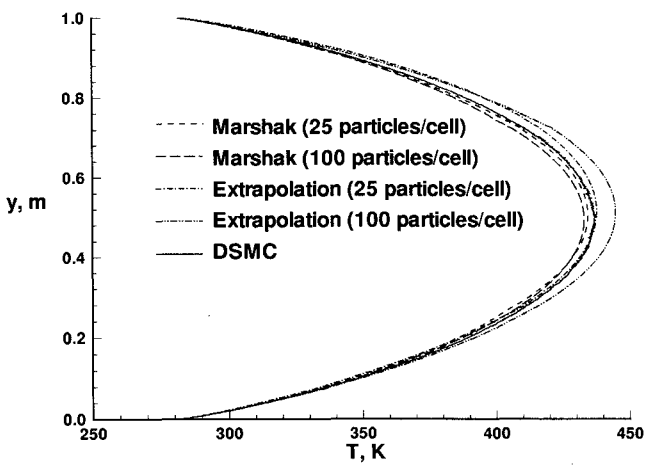

Fig. 10 Temperature profiles for Kn = 0.009 with hybrid coupling every 100 time steps.

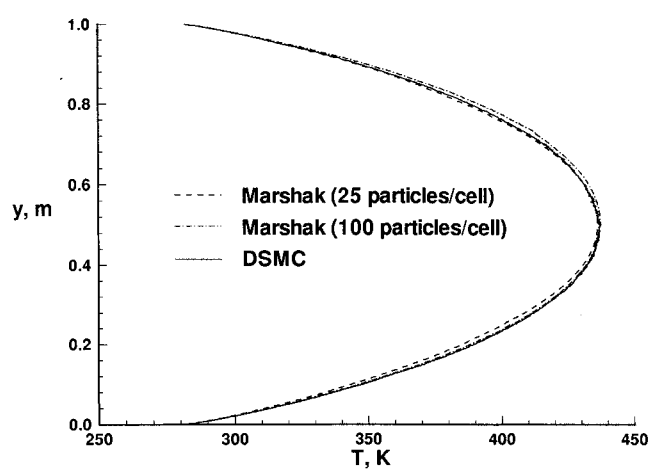

Fig. 11 Temperature profiles for Kn = 0.009 with hybrid coupling every 50 time steps.

Table 2 CPU for various methods, Kn = 0.009

Method	CPU, s (coupling every 50 time steps)	CPU, s (coupling every 100 time steps)	Total no. of simulated particles
Marshak	388.2	385.9	47,000
Property extrapolation	348.6	343.2	47,000
DSMC	555.8	555.8	79,000

The results showed marked improvement as evidenced for the Marshak method in Fig. 11.

Once again, timing measurements were made. These were conducted using 100 particles per cell with hybrid coupling every 50 and 100 time steps. The results are presented in Table 2 for 1000 time steps. Here, the hybrid code produced a much lower speed up than the Kn = 0.003 case of 1.4 for the Marshak condition and 1.6 for the extrapolation technique. Ideally, we would hope for a speed up of 1.7, since 40% less particles are required. However, some amount of overhead is associated with the coupling routine. Some degradation in performance occurs when increasing the frequency of coupling; however, it is very slight, as seen in Table 2.

For this case, the property extrapolation method was faster than the Marshak condition by approximately 10%. It is difficult to explain why the Marshak condition is slower for one Knudsen number and faster in another. Its relative speed to the property extrapolation technique appears to be case dependent.

Conclusions

For the investigations conducted for this work, the Marshak condition offers the best performance in terms of physical accuracy. For the cases considered, the computational time for the Marshak condition was either better or comparable to the property extrapolation technique. The extrapolation of net fluxes proved to be intractable because of difficulties associated with the large degree of scatter in higher moments of the distribution function evaluated from the DSMC method.

The Marshak condition was less affected by the number of simulated particles used than the property extrapolation technique. More importantly, it does not appear to require any more particles per cell than a full DSMC solution. As a result, it is deemed the most advantageous hybrid approach when considering interfaces located in regions of slight translational nonequilibrium.

The use of a Maxwellian distribution for the particles emitted from the Navier–Stokes region provided inaccurate results and should not be used in viscous regions.

Acknowledgments

Support for this work was provided by NASA's Cooperative Agreement NCCI-112 and the Mars Mission Research Center under NASA Grant NAGW-1331. The authors thank Dean Wadsworth, Jeff Taylor, François Mallinger, Patrick Le Tallec, Jens Struckmeier, and Axel Klar, along with Jacques Schneider and Ulrich Giering, for their assistance.

References

[1]Bird, G. A., *Molecular Gas Dynamics and the Direct Simulation of Gas Flows*, Clarendon, Oxford, England, UK, 1994.

[2]Vincenti, W. G., and Kruger, C. H., *Introduction to Physical Gas Dynamics*, Krieger, Malabar, FL, 1965.

[3]Boyd, I. D., Chen, G., and Candler, G. V., "Predicting Failure of the Continuum Fluid Equations in Transitional Hypersonic Flows," AIAA Paper 94-2352, June 1994.

[4]Eggers, J., and Beylich, A. E., "Development of a Hybrid Scheme and Its Application to a Flat Plate Flow," *Rarefied Gas Dynamics 19*, edited by J. Harvey and G. Lord, Vol. 2, Oxford Univ. Press, Oxford, England, UK, 1995, pp. 1216–1222.

[5]Chapman, S., and Cowling, T. G., *The Mathematical Theory of Non-Uniform Gases*, 3rd ed., Cambridge Univ. Press, Cambridge,

England, UK, 1970.
[6]Golse, F., "Applications of the Boltzmann Equation Within the Context of Upper Atmosphere Vehicle Aerodynamics," *Computer Methods in Applied Mechanics and Engineering*, Vol. 75, Oct. 1989, pp. 299–316.
[7]Bourgat, J. F., Le Tallec, P., Tidriri, D., and Qiu, Y., "Numerical Coupling of Nonconservative or Kinetic Models with the Conservative Compressible Navier-Stokes Equations," Rapport de recherche INRIA 1426, France, May 1991.
[8]Bourgat, J. F., Le Tallec, P., Mallinger, F., Tidriri, D., and Qiu, Y., "Numerical Coupling of Boltzmann and Navier-Stokes," *Proceedings of the 6th International Union of Theoretical and Applied Mechanics (IUTAM) Conference on Rarefied Flows for Reentry Problems* (Marseille, France), 1992.
[9]Bourgat, J. F., Le Tallec, P., Mallinger, F., Perthame, B., and Qiu, Y., "Couplage Boltzmann Navier-Stokes," Rapporte de recherche INRIA 2281, France, May 1994.
[10]Wadsworth, D. C., and Erwin, D. A., "One-Dimensional Hybrid Continuum/Particle Simulation Approach for Rarefied Hypersonic Flows," AIAA Paper 90-1690, June 1990.
[11]Wadsworth, D. C., and Erwin, D. A., "Two-Dimensional Hybrid Continuum/Particle Approach for Rarefied Flows," AIAA Paper 92-2975, July 1992.
[12]Eggers, J., and Beylich, A. E., "New Algorithms for Application in the DSMC," *Rarefied Gas Dynamics: Theory and Simulations*, edited by B. Shizgal and D. Weaver, Vol. 159, Progress in Astronautics and Aeronautics, AIAA, Washington, DC, 1994, pp. 166–173.
[13]Illner, R., and Neunzert, H., "Domain Decomposition: Linking Kinetic and Aerodynamic Descriptions," Arbeitsgruppe Technomathematik Bericht 90, Univ. Kaiserslautern, Kaiserslautern, Germany, May 1993.
[14]Klar, A., "Domain Decomposition for Kinetic and Aerodynamic Equations," Dissertation zum Dr. rer. nat., Fachbereich Mathematik, Univ. Kaiserslautern, Kaiserslautern, Germany, July 1994.
[15]Knuth, D. E., *The Art of Computer Programming*, 2nd ed., Addison–Wesley, Reading, MA, 1981.